

# Lawrence Berkeley National Laboratory

## LBL Publications

### Title

CALCULATED AND MEASURED REFLECTIVITY OF ZnGeP<sub>2</sub>

### Permalink

<https://escholarship.org/uc/item/5x304057>

### Authors

Alvarez, Carmen Varea de

Cohen, Marvin L.

Kohn, S.E.

et al.

### Publication Date

1974-07-01

CALCULATED AND MEASURED REFLECTIVITY OF  $\text{ZnGeP}_2$

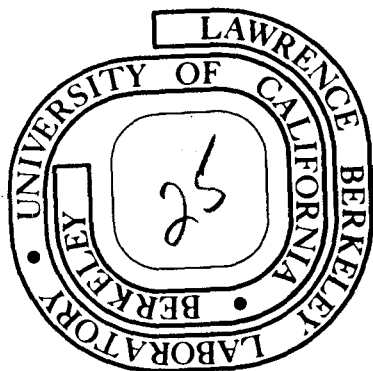
Carmen Varea de Alvarez, Marvin L. Cohen,  
S.E. Kohn, Y. Petroff and Y.R. Shen

July 1974

Prepared for the U. S. Atomic Energy Commission  
under Contract W-7405-ENG-48

TWO-WEEK LOAN COPY

*This is a Library Circulating Copy  
which may be borrowed for two weeks.  
For a personal retention copy, call  
Tech. Info. Division, Ext. 5545*



## **DISCLAIMER**

This document was prepared as an account of work sponsored by the United States Government. While this document is believed to contain correct information, neither the United States Government nor any agency thereof, nor the Regents of the University of California, nor any of their employees, makes any warranty, express or implied, or assumes any legal responsibility for the accuracy, completeness, or usefulness of any information, apparatus, product, or process disclosed, or represents that its use would not infringe privately owned rights. Reference herein to any specific commercial product, process, or service by its trade name, trademark, manufacturer, or otherwise, does not necessarily constitute or imply its endorsement, recommendation, or favoring by the United States Government or any agency thereof, or the Regents of the University of California. The views and opinions of authors expressed herein do not necessarily state or reflect those of the United States Government or any agency thereof or the Regents of the University of California.

Calculated and Measured Reflectivity of ZnGeP<sub>2</sub>

Carmen Varea de Alvarez,<sup>\*†</sup> Marvin L. Cohen,<sup>\*</sup>

S. E. Kohn, Y. Petroff, and Y. R. Shen

Department of Physics, University of California, Berkeley  
and Inorganic Materials Research Division,  
Lawrence Berkeley Laboratory, Berkeley, California 94720

Abstract

Reflectivity spectra of the chalcopyrite ternary compound ZnGeP<sub>2</sub> are studied experimentally and theoretically. The measurements of the reflectivity in both the complete parallel and perpendicular polarizations are made at 5°K. A full zone energy band structure, the reflectivity and imaginary part of the frequency dependent dielectric function are calculated using the empirical pseudopotential method. Comparison is made with the measured reflectivity and modulated reflectivity and prominent features in the experimental spectra are identified and associated with interband transitions. In addition, spin-orbit interactions are included at a few points of the Brillouin Zone.

---

<sup>†</sup>Present address: Plinio 354, Mexico 5, D.F., Mexico.

## I. Introduction

Recently much attention has been given to studies of the electronic and optical properties of ternary chalcopyrite compounds with chemical formula  $A^{N-1}B^{N+1}C_2^{8-N}$  ( $N = 3, 2$ ). We report here the results of experimental and theoretical investigations into the properties of  $ZnGeP_2$ . This material is treated as a model for the chalcopyrite semiconductors. The measurements include detailed reflectivity and modulated reflectivity data for incident light both in the completely parallel and perpendicular polarizations (with respect to the tetragonal axis). Details of the experimental procedures are given in Section II (modulated reflectivity and ordinary reflectivity data are in Figs. 1 and 2 respectively). Theoretical details are in section III. The rest of the paper describes and discusses the results.

Theoretically, the study of the electronic and optical properties of these compounds is a logical extension of the study of their closest analogs the  $B^N C^{8-N}$  ( $N = 3, 2$ ) zincblende semiconductors. The  $A^{N-1} B^{N+1} C_2^{8-N}$  have many interesting physical properties which promise to be useful for studies of the electronic properties of semiconductors in general and for applications to semiconductor technology.

The chalcopyrites also have good non-linear optical properties and have been considered for applications in the infrared.<sup>1</sup> In the case  $N = 3$  most of these ternary compounds crystallize in the chalcopyrite structure which is a simple generalization of the zincblende, crystal structure. We know

from the experimental properties and from the theoretical work of Cohen and Bergstresser,<sup>2</sup> and Phillips and Van Vechten<sup>3</sup> that most of the electronic and optical properties of the  $B^3C^5$  zincblende semiconductors are analogous to those of the diamond structure semiconductors (group  $B^4$ ). Some modifications exist when the effects of the anion and cation difference are introduced into the band structure and bonding properties. In the same way, most of the properties of  $A^2B^4C_2^5$  chalcopyrite semiconductors can be understood by introducing the effects of the differences of the two cations A and B and the small distortion parameter ( $\sigma$ ) of the anion C into the band structure of their zincblende analog. This is done by breaking up the crystalline pseudopotential into a zincblende part and two chalcopyrite modification terms due to the difference between A and B, and the displacement of C. The electronic band structure for  $ZnGeP_2$  is then calculated using the Empirical Pseudopotential Method. In addition, we have calculated the imaginary part of the frequency dependent dielectric function  $\epsilon_2(\omega)$  and the reflectivity spectrum  $R(\omega)$ .

As discussed in section III, pseudopotential form factors for  $ZnGeP_2$  were extracted from GaP form factors<sup>4</sup> and Ge form factors<sup>2</sup> and no experimental information (except lattice parameters) was used to obtain the electronic band structure of this chalcopyrite compound. Spin-orbit interactions were included at a few points of the Brillouin Zone using the method of Weisz<sup>5</sup> as modified by Bloom and Bergstresser.<sup>6</sup>

Comparison of the calculated and measured reflectivity spectra shows that our model gives most of the prominent optical structure but the <sup>calculated</sup> structure is shifted by about 0.3 eV to higher energies. Better agreement can be expected if the form factors are slightly adjusted. This comparison also allows us to identify the interband transitions responsible for the prominent structure in the reflectivity, thus making it possible to extract all the pertinent information that the experimental reflectivity gives on the direct interband transitions.

## II. Experiment

The reflectivity,  $R(\omega)$ , and the logarithmic derivative of the reflectivity,  $1/R dR/d\omega$ , have been measured using our wavelength-modulation spectrometer.<sup>7</sup> The modulating frequency is 1 KHz. Double-beam optics with proper feedback loops were used to eliminate the large unwanted background in the derivative spectrum. Details of the electronic and optical instrumentation have been given elsewhere.<sup>7</sup>

The sample of  $ZnGeP_2$  was a large single crystal obtained from Rockwell International Corp. The crystal was cut parallel to the {100} face. It was then mechanically polished and etched with "Syton." This produced a flat surface with a bluish-metallic appearance. The crystal was then mounted on a copper sample holder and was kept in a helium atmosphere in an optical dewar. This allowed us to work for long periods of time at low temperatures without contamination or deterioration of the surface.

The experimental  $1/R \, dR/d\omega$  spectra at  $5^\circ\text{K}$  are presented in Fig. 1 for light polarized parallel and perpendicular to the C axis of the crystal. For comparison, the modulation spectrum of GaP,<sup>8</sup> the III-V analog of  $\text{ZnGeP}_2$ , is also presented. The reflectivity at  $5^\circ\text{K}$  and at  $300^\circ\text{K}$  for both polarizations is shown in figure 2. As can be seen, the reflectivity spectra are dominated by two main peaks around 3.0 eV and 4.7 eV and a weaker structure at about 3.7 eV. Following the notation of Stokowski<sup>9</sup> for several other II-IV-VI<sub>2</sub> compounds, the two main structures are labeled  $E_1$  and  $E_2$  and the third peak is labeled  $E_c$ . The  $E_1$  and  $E_2$  peaks are composed of several subsidiary structures. Table 1 lists the observed structures along with their experimental and theoretical energies and their assignment to transitions in the Brillouin zone.

### III. Calculations and Results

The pseudopotential Hamiltonian for an electron in the crystal is

$$H = -(\hbar^2/2m)\nabla^2 + V(\underline{r}) \quad (1)$$

where  $V(\underline{r})$  is the weak crystalline pseudopotential that can be expanded in reciprocal lattice vectors  $\underline{G}$

$$V(\underline{r}) = \sum_{\underline{G}} e^{-i\underline{G}\cdot\underline{r}} V(\underline{G})$$

where

$$V(\underline{G}) = \frac{1}{8} \sum_a e^{i\underline{G}\cdot\underline{\tau}_a} V_a(\underline{G}) \quad (2)$$

$\underline{\tau}_a$  is the vector which locates each atom in a primitive cell



and  $V_a(G)$  is the fourier transform of the atomic pseudo-potential for atoms of kind a, which is assumed spherically symmetric.

$$V_a(G) = \frac{1}{\Omega} \int V_a(\vec{r}) e^{i\vec{G}\cdot\vec{r}} d^3r \quad (3)$$

$\Omega$  is the atomic volume.  $ZnGeP_2$  crystalizes in a body-centered tetragonal structure with 8 atoms in the primitive cell; the basis is given by

$$\begin{aligned} \text{Zn: } \tau_1^{\text{Zn}} &= (0,0,0), & \tau_2^{\text{Zn}} &= (0,a/2,c/4) \\ \text{Ge: } \tau_1^{\text{Ge}} &= (0,0,c/2), & \tau_1^{\text{Ge}} &= (0,a/2,3c/4) \\ \text{P: } \tau_1^{\text{P}} &= (au,a/4,c/8), & \tau_2^{\text{P}} &= (a\bar{u},3a/4,c/8), \\ \tau_2^{\text{P}} &= (3a/4,au,7c/8), & \tau_4^{\text{P}} &= (a/4,a\bar{u},7c/8) \end{aligned}$$

where  $a = 5.46\text{\AA}$ ,  $c = 10.71\text{\AA}$ ,  $u = 0.2582$  at room temperature.<sup>10</sup>

The space group is the non-symmorphic group  $D_{2d}^{12}$  (body centered tetragonal lattice) and the unit cell (see Fig. 3) can be thought of as composed of two zincblende unit cells (volume  $a^3$ ) stacked and compressed along the z-axis. A primitive cell of the chalcopyrite structure (volume  $ac^2/2$ ) contains 4 primitive cells of the zincblende (volume  $a^3/4$ ). The cation of the zincblende is substituted by the two cations of the chalcopyrite in such a way that two kinds of chains are formed Zn-P-Ge-P-Zn chains run along the  $(1,\pm 1,0)$  directions while Zn-P-Zn-P-Ge-P-Ge-P-Zn chains run along the  $(0,\pm 1,1)$  and  $(\pm 1,0,1)$  directions. The presence of Zn-P-Zn and Ge-P-Ge linkages along the z-axis is responsible for the doubling of the unit cell with respect to the zincblende case. The lattice is slightly compressed along the z-axis, this

tetragonal compression being measured by the parameter  $\epsilon = 2-c/a$ . The anion of  $ZnGeP_2$  is tetrahedrally coordinated to two Zn and two Ge atoms and slightly displaced from the centers towards the smaller pair of cations (the Ge atoms); this displacement can be measured by the small parameter  $\sigma = 4u-1$ . The zincblende and the chalcopyrite structures are similar. The first Brillouin zone of the chalcopyrite can be obtained by folding down the first Brillouin zone of the zincblende (see Fig. 4). The  $\tilde{G}$  vectors used in the folding in process are  $\tilde{\Gamma} = (0,0,0)$ ,  $\tilde{W}_x = (1,0,1)$ ,  $\tilde{W}_y = (0,1,1)$  and  $\tilde{X}_z = (0,0,2)$ .<sup>11</sup> It is easy to show that the set of  $\tilde{G}$  vectors of the chalcopyrite structure can be broken into four different sets of the form  $\tilde{G} = \tilde{G}_{zb} + \tilde{\Gamma}$ ,  $\tilde{G} = \tilde{G}_{zb} + \tilde{W}_x$ ,  $\tilde{G} = \tilde{G}_{zb} + \tilde{W}_y$  and  $\tilde{G} = \tilde{G}_{zb} + \tilde{X}_z$ .

Some of the ternary crystals with composition  $A^2B^4C^5$  (e.g.  $MgGeP_2$ ), lack the segregation of their two cations. The cations are considered randomly distributed among the cation position in the zincblende analog. Then the compound has the zincblende structure; one of the two sites in the primitive cell is occupied by the anion and the other by an average of the two cations  $(A^2+B^4/2)$ . It is mainly the ordering of the two cations and their different potentials which distinguishes the chalcopyrite from the zincblende (zb) structure. In view of this, it is instructive to decompose the crystalline pseudopotential in reciprocal space (Eq. 2) into a zb component which includes the average of the two cation potentials and another which takes into account

the modification due to the chalcopyrite structure.

$$V_1(G) = (V_{Zn}(G) + V_{Ge}(G))/2$$

$$V_2(G) = V_P(G)$$

$$V_A^C(G) = (V_{Zn}(G) - V_{Ge}(G))/2 \quad (4)$$

where  $V_1$  is the average and  $2V_A^C$  is the difference of the two cation potentials. We also define the vectors  $\beta_i$  ( $i = 1,4$ ) to specify the displacement of the anions:

$$\begin{aligned} \beta_1 &= \tau_1^P - \sigma_1, & \beta_2 &= \tau_2^P + \sigma_2 \\ \beta_3 &= \tau_3^P - \sigma_3, & \beta_4 &= \tau_4^P + \sigma_4 \end{aligned}$$

where  $\sigma_1 = (\sigma, 0, 0)a/4$ ,  $\sigma_2 = -\sigma_1$ ,  $\sigma_3 = (0, \sigma, 0)a/4$  and  $\sigma_4 = -\sigma_3$  represent the displacement of the P atoms from their original sites in the zb analog. With this, Eq. (2) can be written in the form:

$$\begin{aligned} V(\tilde{G}) &= \frac{1}{8} V_{Zn}(G) \sum_{i=1}^2 e^{i\tau_i^{Zn} \cdot \tilde{G}} + \frac{1}{8} V_{Ge}(G) \sum_{i=1}^2 e^{i\tau_i^{Ge} \cdot \tilde{G}} \\ &+ \frac{1}{8} V_2(G) \sum_{i=1}^4 e^{i\tau_i^P \cdot \tilde{G}} \\ &= \frac{1}{8} V_1(G) \left( \sum_{i=1}^2 e^{i\tau_i^{Zn} \cdot \tilde{G}} + \sum_{i=1}^2 e^{i\tau_i^{Ge} \cdot \tilde{G}} \right) \\ &+ \frac{1}{8} V_2(G) \sum_{i=1}^4 e^{i\beta_i \cdot \tilde{G}} \\ &+ \frac{1}{8} V_A^C(G) \left( \sum_{i=1}^2 e^{i\tau_i^{Zn} \cdot \tilde{G}} - \sum_{i=1}^2 e^{i\tau_i^{Ge} \cdot \tilde{G}} \right) \\ &+ \frac{1}{8} V_2(G) \sum_{i=1}^4 e^{i\beta_i \cdot \tilde{G}} (e^{i\sigma_i \cdot \tilde{G}} - 1) \end{aligned} \quad (5)$$

As is customary in the zb case, let us define

$$V_S(G) = [V_1(G)+V_2(G)]/2 = [V_{Zn}(G)+V_{Ge}(G)+2V_P(G)]/4$$

and

$$V_A(G) = [V_1(G)-V_2(G)]/2 = [V_{Zn}(G)+V_{Ge}(G)-2V_P(G)]/4 \quad (6)$$

We then have, from the first two terms on the right hand side of Eq. (5) the zb part of the potential:

$$V_{zb}(G) = e^{iG \cdot \eta} [S_S(G)V_S(G) + iS_A(G)V_A(G)]$$

Here, the structure factors  $S_S(G)$  and  $S_A(G)$  are the usual symmetric and antisymmetric structure factors of the zb (compressed along the c-axis) structure; the phase factor  $e^{iG \cdot \eta}$  only shifts the origin to the Zn atoms (the usual origin in the zb case is half way between the two atoms in the cell).

Since it is expected that the electronic properties of  $ZnGeP_2$  should closely resemble those of its zb analog, GaP, in the present calculation we used  $V_S(G) = V_S^{GaP}(G)$  and  $V_A(G) = V_A^{GaP}(G)$ . The GaP form factors used were obtained from ref. 4, the Ge form factors used from ref. 2, and the Zn and P form factors extracted from Eqs. (6). The pseudopotential curves of  $V_i(|G|)$  versus  $|G|$  were free hand extrapolated and renormalized to the atomic volume of  $ZnGeP_2$  (see Eq. (3)).

The third term on the right hand side of Eq. (5) which is due to the difference between the potentials of the two cations, can be written in the form

$$V_a^c(G) = S_A^c(G)V_A^c(G) \quad (7)$$

The structure factor  $S_A^c(\underline{G})$  can be reduced to the form (see Eq. (5))

$$S_A^c(\underline{G}) = -\frac{i}{2} e^{i\tau_2 \cdot \underline{G}} \sin(\tau_1 \cdot \underline{G}) \cos(\tau_2 \cdot \underline{G}) \quad (8)$$

The last term on the right hand side of Eq. (5) is due to the displacement of the anion and depends only on the pseudopotential form factors of the anion and on the distortion parameter  $\sigma$ . We put the term in the form

$$V_u(\underline{G}) = V_p(\underline{G}) S_u(\underline{G}) \quad (9)$$

where the structure factor  $S_u(\underline{G})$  is

$$S_u(\underline{G}) = \frac{1}{8} \sum_{i=1}^4 e^{i\beta_i \cdot \underline{G}} (e^{i\sigma_i \cdot \underline{G}} - 1) \quad (10)$$

Since  $\sigma \sim 0.1$  for most of the  $A^2B^4C_2^5$  chalcopyrite compounds in which the  $u$  parameter has been measured, Eq. (10) shows that the structure factors  $S_u(\underline{G})$  are small in the region in reciprocal space where the pseudopotentials are appreciably different from zero [ $|\underline{q}| \leq 4(2\pi/a)$ ]. From the above it should be clear that the effects of  $V_u(\underline{G})$  on the band structure are expected to be small. On the other hand, the non-zero  $S_A^c(\underline{G})$  are of the order of one fourth of the non-zero  $S_S(\underline{G})$  or  $S_A(\underline{G})$ .

One can understand the band structure of the chalcopyrite compounds as a modification of the band structure of their zincblende analogs. To do that one proceeds as follows:

(1) the band structure of the zincblende analog is first folded into the smaller chalcopyrite Brillouin zone. (2) In the fold-in process, each  $\underline{k}_{\text{chal}}$  vector in the first chalcopyrite BZ corresponds to four different  $\underline{k}_{\text{zb}}$  vectors in the

first zincblende BZ. (3) In "turning on" the "chalcopyrite perturbation," the states at  $\tilde{k}$ ,  $\tilde{k}+\tilde{W}_x$ ,  $\tilde{k}+\tilde{W}_y$  and  $\tilde{k}+\tilde{X}_z$  in the zincblende BZ are mixed. Since  $S_A^C(\tilde{G})$  is non-zero only for  $\tilde{G} = \tilde{G}_{zb} + \tilde{W}_x$  or  $\tilde{G} = \tilde{G}_{zb} + \tilde{W}_y$ , the pseudopotential  $V_a^C(\tilde{G})$  mixes only those  $\tilde{k}$  states that differ by  $\tilde{W}_x$  or  $\tilde{W}_y$ . One expects big changes in the band structure at points such as the crossing point of the W-L and  $\Gamma$ - $\Sigma$  lines in the conduction band along the  $\Sigma$  direction of the chalcopyrite BZ or at  $X[\Sigma(1/2,1/2,0),L]$  at the top of the valence band where the energies of the  $\Sigma_2$  and  $L_3$  levels are very close to each other. (4) The structure factors  $S_u(\tilde{G})$  are non-zero for all the four subsets of  $\tilde{G}$ , but we have shown that the pseudopotential  $V_u(\tilde{G})$  is expected to be small, and so, the mixing of  $\tilde{k}$  and  $\tilde{k}+\tilde{X}_z$  states should be small. One of the consequences is that the  $\Gamma_4+\Gamma_5(\Gamma_{15})-\Gamma_3(X_1)^{12}$  pseudo-direct transitions<sup>14,15</sup> are very weak. These transitions are only observable by optical modulation techniques when they constitute the first absorption edge of the crystal.<sup>14,16</sup>

In solving for the eigenvalues and eigenvectors of the full Hamiltonian, we expanded the wave functions into a set of 69-84 plane waves; 244 additional plane waves were used through the perturbation scheme developed by Lowdin.<sup>17</sup> The energies and wave functions were calculated in 1/16 of the BZ at 288 grid points, and the  $\epsilon_2(\omega)$  integration over  $k$ -space was performed by the method developed by Gilat and Raubenheimer<sup>18</sup> in what we call the practical Brillouin zone (PBZ). The PBZ was chosen because it can easily be

shown that the region in k-space surrounded by the planes  $k_z = 0$ ,  $k_z = 2\pi/c$ ,  $k_z = k_y$ ,  $k_y = 0$  and  $k_z = \pi/a$  is completely equivalent to the usual irreducible part of the BZ (i.e. 1/16 of the full BZ).

Spin-orbit corrections were carried out at a few points in the BZ by extending the zincblende calculation.<sup>5,6</sup> The fact that we are dealing with three kinds of atoms and 8 atoms in the primitive cell presents no problem. We use the 2 ratios of the cations to the anion spin-orbit contributions given in Ref. 19; this leaves us with one-spin orbit parameter which we choose to be that of Ge. The usual procedure is to fit this parameter to the spin-orbit splitting  $\Delta_{s0}$  at the  $\Gamma$  point of the BZ. At the time this calculation was performed, there was no experimental information about  $\Delta_{s0}$  for  $\text{ZnGeP}_2$ , so the parameter we chose was the one that gives the correct spin-orbit splitting for Ge in the diamond structure. The eigenvalues of the spin orbit Hamiltonian require the diagonalization of a  $138 \times 138$  matrix and the large amount of computer time involved prohibits spin-orbit calculations over the entire BZ.

#### A. Optical Structure in the $E_0$ Region

The first optical transitions in  $\text{ZnGeP}_2$  are transitions from the top of the valence band to the bottom of the conduction band at  $\Gamma$ . The  $\Gamma_{15}$  valence band in GaP is split by the crystal field splitting  $\Delta_{cr}$  into a doubly degenerate band of  $\Gamma_5$  symmetry and a singlet band of  $\Gamma_4$

symmetry. With the addition of spin-orbit interactions, the  $\Gamma_5$  states split into states of  $\Gamma_{\bar{1}}$  and  $\Gamma_{\bar{2}}$  symmetry. The first optical transitions with significant oscillator strength are from these three valence band states to a conduction band of  $\Gamma_{\bar{1}}$  symmetry which is the analog of the  $\Gamma_1$  states in GaP. These transitions, labeled A, B, and C, have been seen and discussed by Shay<sup>14</sup> and by Shileika.<sup>16</sup> In room temperature electroreflectance Shay observes these transitions at 2.34 eV, 2.40 eV and 2.48 eV respectively. Shileika reports values of 2.46 eV, 2.53 eV and 2.59 eV also from room temperature electroreflectance. At 5°K we observe structures at 2.51 eV, 2.63 eV and 2.67 eV, and we tentatively assign the latter two to B and C. From these values, we calculate values for the spin-orbit splitting of  $\Delta_{s0} = 0.13$  eV and for the crystal field splitting of  $\Delta_{cr} = -0.04$  eV using the quasi-cubic theory of Hopfield.<sup>20</sup> In our pseudopotential calculation of the ZnGeP<sub>2</sub> band structure, we have used the spin-orbit parameter  $\Delta_{s0} = 0.16$  eV for Ge. We find these transitions at 2.31 eV, 2.27 eV and 2.43 eV respectively. The centroid of this triplet, 2.34 eV, is shifted approximately 0.3 eV from the centroid of the experimental energies, which appears to be general for all of the pseudopotential critical point energies we calculate for ZnGeP<sub>2</sub>. In the more rigorous calculation, we should use the experimental  $\Delta_{s0}$  as a known parameter. The theoretical value of the B peak is less than that of the A peak because we predict a positive crystal field splitting, while the experimental value is negative. First order perturbation



predicts that this quantity depends only on the tetragonal compression of the crystal, and therefore it depends only on the slopes of the pseudopotential curves near the reciprocal lattice vectors  $(2,0,0)$ ,  $(2,2,0)$  and  $(3,1,2)$ . Since the crystalline tetragonal compression is so small, form factors have to be determined to the third significant figure.

Therefore  $\Delta_{cr}$  is difficult to predict. It would however be easy to adjust the pseudopotential curves to give the correct crystal field splitting.

The zincblende analog of  $ZnGeP_2$  is an indirect gap  $\Gamma_{15}-X_1$  semiconductor. When the BZ of GaP is folded into the BZ of  $ZnGeP_2$ , the  $X_1$  states of GaP map into  $\Gamma$  states of  $ZnGeP_2$ . Furthermore, the effect of  $V_A^c(\vec{G}) + V_u(\vec{G})$  is expected to be small near the band edge at  $\Gamma$  because the  $\Gamma(W)$  states are far away from the band gap in GaP. Thus it is expected that <sup>the</sup> lowest interband transition in  $ZnGeP_2$  will have a very small oscillator strength, and  $ZnGeP_2$  is referred to as a "pseudodirect" gap semiconductor. Moreover, the hydrostatic pressure coefficient is expected to be close to that of the  $\Gamma$ -X edge of  $GaP^{21}$  since this parameter depends only on the symmetry of the wave functions which are almost unaffected by the chalcopyrite potential. All of this has been observed for  $ZnGeP_2$ . Shileika<sup>16</sup> observes very weak transitions at 2.14 eV and 2.21 eV, labeled B' and C', in wavelength modulated absorption at 77°K. These are assigned to transitions from the spin orbit split  $\Gamma_5$  valence band to the  $\Gamma_3$  conduction band. He also observes the band gap at

2.08 eV with a hydrostatic pressure coefficient of  $2.2 \times 10^{-6}$  eV kg<sup>-1</sup> cm<sup>2</sup>. In electrodiffractance, Shileika observes very weak structure at 2.3 eV which is attributed to transitions  $\Gamma_5-\Gamma_2$ , the analog of the  $\Gamma_{15}-X_3$  transition in GaP. Shay observes the B' and C' structures at 2.05 eV and 2.11 eV. In our measurements at 5K, we observe a small structure at 2.14 eV in both polarizations which agrees well with the results of Shileika. We also observe weak structures at 2.29 eV for perpendicular polarization and 2.31 eV for the parallel polarization. We believe these are the B'' and C'' transitions seen by Shileika.

#### B. Optical Structure in the $E_1$ Region

As shown in Fig. 1, the experimental modulated reflectivity of ZnGeP<sub>2</sub> shows much richer structure than that of its analog (GaP). In the  $E_1$  region corresponding to the two spin-orbit split peaks,  $E_1$  and  $E_1+\Delta_1$  of GaP, ZnGeP<sub>2</sub> has five resolvable structures. In general these splittings are observed in most of the chalcopyrite compounds studied so far.<sup>22</sup> These five structures in the spectrum have been labeled  $E_1(1)$ ,  $E_1(2)$ ,  $E_1(3)$ ,  $E_1(4)$  and  $E_c$  by Stokowski<sup>9</sup> and  $E_1$ ,  $E_2$ ,  $E_3$ ,  $E_4$ ,  $E_6$  by Shileika.<sup>16</sup> We will stick to Stokowski's notation. The most important features of these structures are the following, the energy separations  $E_1(2)-E_1(1)$  and  $E_1(3)-E_1(4)$  are close to each other for most of the  $A^2B^4C_2^5$  crystals studied, this seems to indicate that the first four transitions in the  $E_1$  region come from two spin-orbit split

doublets in the same region of the BZ. Both our experimental results and critical point analysis show that this is not the case at least for  $\text{ZnGeP}_2$ . The experimental splitting  $E_1(2)-E_1(1)$  is 0.06 eV while the  $E_1(4)-E_1(3)$  splitting is 0.21 eV. The origin of these structures has been subject to extensive investigation in the last few years. Most interpretations agree in that the  $E_1(1)$  and  $E_1(2)$  structure originates from transitions in the N-plane along the  $2\pi(x/a, x/a, 2x/c)$  direction. This is equivalent to the  $\Lambda$  transitions in GaP when one uses a quasicubic model. Our full zone calculations for the reflectivity of  $\text{ZnGeP}_2$ , show that this is indeed the case and the critical point is near  $x = 0.2$  (Fig. 4). We find that the mixing of the valence bands involved in the transitions under the action of the chalcopyrite part of the pseudopotential is very small, so spin-orbit interaction effects should be very close to those of GaP. Our calculated spin-orbit splitting between the  $E_1(1)$  and  $E_1(2)$  peaks is  $\Delta_1 = 0.08$  eV. In the experimental modulated spectrum its value is  $\Delta_1 = 0.06$  eV.

The nature of the  $E_1(3)$  and  $E_1(4)$  structure is more subject to controversy. Kavaliauskas et al.<sup>23</sup> suggest that all four peaks  $E_1(1)$  to  $E_1(4)$  come from transitions at the X point of the BZ in the bands 15-16 (top valence band)  $\rightarrow$  17-18 (bottom conduction band) and 13-14  $\rightarrow$  17-18. Under the influence of the spin-orbit interactions, each four fold degenerate level  $X_1$ , splits into two two-fold degenerate levels  $X_1 \rightarrow X_1^- + X_4^-$ ,  $X_2^- + X_3^-$ . From our studies in  $\text{ZnGeP}_2$ ,

the splitting  $X_1 + X_4 - X_2 + X_3$  is 0.02 eV. It is thus too small to be associated with the energy separation between  $E_1(1)$ ,  $E_1(3)$  and  $E_1(2)$ ,  $E_1(4)$  as Kavaliauskas et al. suggest. Stokowski<sup>9</sup> assigns the  $E_1(3)$  and  $E_1(4)$  peaks to transitions at the X point of the BZ, the top of the valence band at the X point of the BZ contains six levels (11-16) which are almost degenerate in a quasi cubic model. These six levels correspond to the two four-fold degenerate levels  $X_1(L_3)$  [ $L_3 = (1/2, -1/2, -1/2)2\pi/a$  and  $L_3 = (-1/2, 1/2, -1/2)2\pi/a$ ] and the four-fold degenerate level  $X_1(\Sigma_1)$  [ $\Sigma_1 = (1/2, 1/2, 0)2\pi/a$ ,  $\Sigma_1 = (-1/2, -1/2, 0)$ ]. The fact that the  $L_3$  and  $\Sigma_1$  levels are almost degenerate is not accidental. Cohen and Bergstresser's<sup>2</sup> band structures for the  $B^N C^{8-N}$  semiconductors show that the  $L_3$  and  $\Sigma_1$  levels are always very close in energy. Under these circumstances, the effects of the chalcopyrite part of the pseudopotential mixing the  $\Sigma_1$  and  $L_3$  levels is expected to be large as shown in Fig. 4. This large interaction and the shifts of  $L_3^v$  to  $L_1^c$  transitions relative to the  $\Lambda_3^v$  to  $\Lambda_1^c$  transitions, underlie the Stokowski<sup>9</sup> suggestion that the  $E_1(3)$ ,  $E_1(4)$  and  $E_c$  peaks come from transitions at the X point from bands (11,12), (13,14), (15,16)  $\rightarrow$  (17,18). Even though all of these transitions are allowed due to the strong L- $\Sigma$  mixing in the valence band, we find that the (15,16)  $\rightarrow$  (17,18) transitions at the X point lay below the  $\Lambda[E_1(1), E_1(2)]$  peak. The  $X_1 - X_1$  transitions [bands (15,16)  $\rightarrow$  (17,18)] make some contributions to the  $E_1(1)$  peak of our calculated

$\epsilon_2(\omega)$  (see Fig. 5), and the  $X_1-X_1$  transitions [bands (13-14) + (17,18)] contribute to the  $E_1(2)$  peak of our calculated  $\epsilon_2(\omega)$ .

In the region corresponding to the  $E_1(3)$  and  $E_1(4)$  peaks of the experimental reflectivity, we find two pieces of structure mostly in the perpendicular polarization; we find that these two structures come mainly from transitions in the N-plane of the BZ. One critical point is close to the point (0.3,0.3,0.38) (bands 16-17) and the other is close to (0.25,0.25,0) (bands 16-18). These two critical points have the same origin in a quasi-cubic model. A plot of the folded in band structure of a zincblende semiconductor, shows that the (0,0,0) to (1/2,1/2,z) line and the (1,0,1) to (1/2,-1/2,z-1) line in the first conduction band always cross along a line close to the (1/4,1/4,0) to A(1/2,1/2,1/2) direction; the interaction between these lines is quite strong creating the two critical points mentioned above.

We have been able to associate the  $E_c$  structure to transitions at the X point  $X_1(\Sigma_2, L_3) \rightarrow X_1(L_1)$ , this peak is stronger in the parallel polarization. One has to be cautious when identifying the  $E_c$  structure, since it is caused by an  $M_0$  singular point; the actual peak is shifted by about 0.1 eV to higher energies with respect to the energy of the transition at the singularity.

C. Optical Structure in the  $E_2$  Region

At higher energies, in the region corresponding to the  $E_2$  peak of the reflectivity structure of zincblende semiconductors, at least five pieces of structure are observed. In the measured modulated reflectivity of  $\text{ZnGeP}_2$ , we have been able to identify six prominent pieces of structure. Our calculations show that most of the contribution to the  $E_2$  structure comes from transitions in the  $\Delta$  and  $\Sigma$  directions of the zb analog as expected. The  $\Delta$  direction folds into the  $\Delta$ ,  $\Lambda$  and  $(1-x,0,1)$  directions of the chalcopyrite BZ, while the  $\Sigma$  direction is folded into the  $\Sigma$ ,  $(x,0,2x)$  and  $(1-x,0,2x-1)$  directions. Summation over k-space along  $\Delta$  and  $\Sigma$  directions shows that in effect the  $E_2$  peak is mainly a  $\Delta$ ,  $\Sigma$  peak.

The first peak in the parallel polarization around 4.76 eV comes from transitions along the  $\Delta$  direction (15-17) at  $(0.34,0,0)$ ; the line  $\Delta(\Delta)$  mixes with the line  $\Delta(1-x,0,1/2)$  in the valence band and then continues into bands (13,14), so transitions  $(13,14) \rightarrow 17$  near  $(0.5,0,0)$  also contribute to this peak. In the experimental spectra this peak is at 4.3 eV. On the other hand,  $\Lambda(0,0,x)$  and  $\Sigma$  transitions are responsible for the first peak in the  $\Delta$  perpendicular polarization at 4.77 eV; the corresponding experimental peak is at 4.46 eV. The bands involved in this transition are 12,13-18 and the critical point is near  $\Gamma_5(X_5) - \Gamma_3(X_1)$ . The main peak in the perpendicular polarization is caused by  $\Sigma$  transitions near the point X, bands 16-20, indicating the strong

mixing of  $\Sigma$  and L at X in the valence bands. Our calculated peak is at 4.96 eV while experiment shows it at 4.79 eV. The small shoulder at 4.6 eV, (4.17 eV in the experiment) in the  $\perp$  polarization is caused by a singular point at (0,0,0.6) along the  $\Lambda$  direction (bands 13-17). In this energy region we also find a critical point at (0.25,0.25,0) (14 $\rightarrow$ 17 transitions) coming from the original  $\Sigma$  transitions of the zb analog, these transitions are allowed only in the perpendicular polarization.

The main peak in the parallel polarization is caused by a strong critical point near (0.16,0.5,0), from bands (14-17). In this energy region we find two additional pieces of structure caused by a critical point at (0.25, 0.25,0.5) in the N plane from bands 13-18 and 14-20. One structure at 5 eV appears in the parallel polarization while the other at 5.11 eV appears in the perpendicular direction. The shoulder at 4.92 eV in the experimental spectrum is associated with  $\Delta(0.5,0,0)$  transitions from bands 15-18; our calculated value for these transitions is 5.21 eV.

#### IV. Discussion

Table 1 shows the results of the critical point analysis and a comparison with the experiment. As shown in Fig. 4, the strength of the  $E_2$  peak of  $\text{ZnGeP}_2$  is considerably reduced when compared with the strength of the same peak in zincblende semiconductors. It is still higher than the measured peak, which appears to have the same strength as the  $E_1$  peak.

This, together with the fact that the width of the  $E_2$  peak is about 0.8 eV while our calculation shows a width of about 0.4 eV, indicates that we probably underestimated the anti-symmetric cation potential for this calculation. In most other respects the structure in the experiment is very similar to our theoretical predictions. We note that by shifting the theoretical spectra by about 0.3 eV to lower energies the agreement between theory and experiment for almost all the optical structure is very good. This suggests that small changes in the form factors could give theoretical spectra in excellent agreement with experiment. This is encouraging since no experimental data (except for structure constants) were used in carrying out the calculations.

#### Acknowledgment

We would like to thank Dr. Roger DeWames of Rockwell International Corp. for the large crystal of  $ZnGeP_2$ . Part of this research was done under the auspices of the Atomic Energy Commission.



References

- \* Supported in part by the National Science Foundation Grant GH 35688.
1. G. D. Boyd, E. Buehler, F. G. Storz and J. H. Wernick, J. of Quantum Electronics QE-8, 419 (1972).
  2. M. L. Cohen and T. K. Bergstresser, Phys. Rev. 141, 789 (1966).
  3. J. C. Phillips and J. A. Van Vechten, Phys. Rev. B2, 2147 (1970).
  4. J. P. Walter and M. L. Cohen, Phys. Rev. 183, 763 (1969).
  5. G. Weisz, Phys. Rev. 149, 504 (1966).
  6. S. Bloom and T. K. Bergstresser, Solid State Comm. 6, 4651 (1968).
  7. R. R. L. Zucca and Y. R. Shen, Applied Optics 12, 1293 (1973); Y. R. Shen, Surface Science 37, 522 (1973).
  8. C. Varea de Alvarez, J. P. Walter, M. L. Cohen, J. Stokes, and Y. R. Shen, Phys. Rev. B6, 1412 (1972).
  9. S. E. Stokowski, Phys. Rev. B6, 1294 (1972).
  10. R. DeWames, private communication.
  11. The x and y components of the  $\tilde{G}$  and  $\tilde{k}$  vectors are in units of  $2\pi/a$  and the z components in units of  $2\pi/c$  throughout this work.
  12. Often in this work we denote a state by its symmetry in the chalcopyrite structure (group  $D_{2d}^{12}$ , see Ref. 13) and in parenthesis the symmetry of the zb state where it originates from in a perturbation approach.

13. S. Zak, The Irreducible Representations of Space Groups (Benjamin, New York, 1969).
14. J. L. Shay, B. Tell, E. Buehler and J. H. Wernick, Phys. Rev. Lett. 30, 983 (1973).
15. J. E. Rowe and J. L. Shay, Phys. Rev. B3, 451 (1971).
16. R. A. Bendorius, G. Z. Krivaite, A. Yu. Shileika, G. F. Karavaev, and V. A. Chaldyshev, International Conference on Semiconductors, Warsaw (1972) (to be published); A. Raudonis, V. S. Grigoreva, V. D. Prochukhan and A. Shileika, Phys. Stat. Solidi (b) 57, 415 (1973); A. Shileika, Surface Sci. 37, 730 (1973).
17. P. Löwdin, J. Chem. Phys. 19, 1396 (1951).
18. G. Gilat and L. J. Raubenheimer, Phys. Rev. 144, 390 (1966).
19. F. Herman and S. Skillman, Atomic Structure Calculations (Prentice Hall, Englewood Cliffs, N.J. 1966).
20. J. J. Hopfield, J. Phys. Chem. Solids 15, 97 (1960).
21. W. Paul, in Proceedings of the Colloquium on the Physical Properties of Solids under Pressure, Grenoble, 1969 (Centre National de la Recherche Scientifique, Grenoble, 1970), p. 199.
22. J. L. Shay, E. Buehler, and J. H. Wernick, Phys. Rev. B2, 4104 (1970) and Phys. Rev. B3, 2004 (1971); J. L. Shay and E. Buehler, Phys. Rev. B3, 2598 (1971) and Phys. Rev. B4, 2479 (1971); C. C. Y. Kwan and J. C. Woolley, Canad. J. Phys. 48, 2085 (1970); Phys. stat. sol. (b) 44, K93 (1971); Appl. Phys. Letters 18, 520 (1971); R. K. Karymshakov, Y. I. Ukhanov, and Y. V.

Shmartsev, Fiz. Tekh. Poluprov. 5, 514 (1971) [Sov. Phys.-Semiconductors 5, 450 (1971)].

23. J. Kavaliauskas, G. F. Karavaev, E. I. Leonov, V. M. Orlov, V. A. Chaldyshev and A. Shileika, Phys. stat. sol. (b) 45, 443 (1971).

Table Caption

Table I. Theoretical and experimental reflectivity structure and their identifications, including the location in the Brillouin zone and energy of the calculated critical points for  $\text{ZnGeP}_2$ .

Table I  
Reflectivity structure

Theoretical Peak Position (eV)	Experimental Peak Position (eV)				Polarization (a)	Peak	Location in zone	cp energy (eV)
	(a)	(b)	(c)	(d)				
		2.08†				A'	$\Gamma_4-\Gamma_3$	
	2.14	2.145†	2.05		, I	B'	$\Gamma_5-\Gamma_3$	
		2.21†	2.11			C'		
	2.29				I	B''		
	2.31	2.3†				C''	$\Gamma_5-\Gamma_2$	
2.31	2.51	2.46	2.39	2.34	, I	A	$\Gamma_2-\Gamma_1$	2.31*
2.27	2.63	2.53	2.46	2.40	I	B	$\Gamma_1-\Gamma_1$	2.27*
2.43	2.67	2.59	2.52	2.48			C	$\Gamma_2-\Gamma_1$
3.04						$E_1(1)$	$X_1-X_1(15,16-17,18)$	3.04 { 3.05* 3.03*
3.41	3.02	3.02	2.97	2.87 (2.92)	, I		$N_1-N_1(16-17)$ (0.2,0.2,0.4)	3.42*
3.37					I	$E_1(2)$	$X_1-X_1(13,14-17,18)$	3.36 { 3.35* 3.37*
3.41	3.08	3.15	3.09	3.05	I,		$N_2-N_1(15-17)$ (0.2,0.2,0.4)	3.50*
3.6	3.2	3.22	3.13	3.32	I(II)	$E_1(3)$	$N_2-N_1(16,17)$ (0.3,0.3,0.38)	3.6
3.9	3.41	3.48	3.41	3.64	I	$E_1(4)$	$\Sigma_2-\Sigma_1(16,18)$ (0.25,0.25,0)	3.95

Table I (continued)

Theoretical Peak Position (eV)	Experimental Peak Position (eV)				Polarization (a)	Peak	Location in zone	cp energy (eV)
	(a)	(b)	(c)	(d)				
4.0	3.74 (3.72)	3.75	3.71	3.83	( $\perp$ )	$E_c$	$X_1-X_1(11,12-17,18)$	3.9
4.6	4.17				$\perp$		$\Lambda(13-17)(0,0,0.6)$ $\Sigma(14-17)$ (0.25,0.25,0)	4.6
4.76	4.3						$\Delta(15-17)(0.34,0,0)$	4.76
4.77	4.46				$\perp$	$E_2$	$\Gamma-\Gamma(13-18)$	4.77
5.05	4.73						(14-17)(0.16,0.5,0)	5.05
4.96	4.79				$\perp$		X(16-20) and along $\Sigma$	4.96
5.21	4.92	(4.93)			( $\perp$ )		$\Delta(15-18)(0.5,0,0)$	5.21

(a) This work at 5°K

(b) Thermoreflectance work of Shileika at 120°K (Ref. 16)

(c) Electromoreflectance work of Shileika at 300°K (Ref. 14)

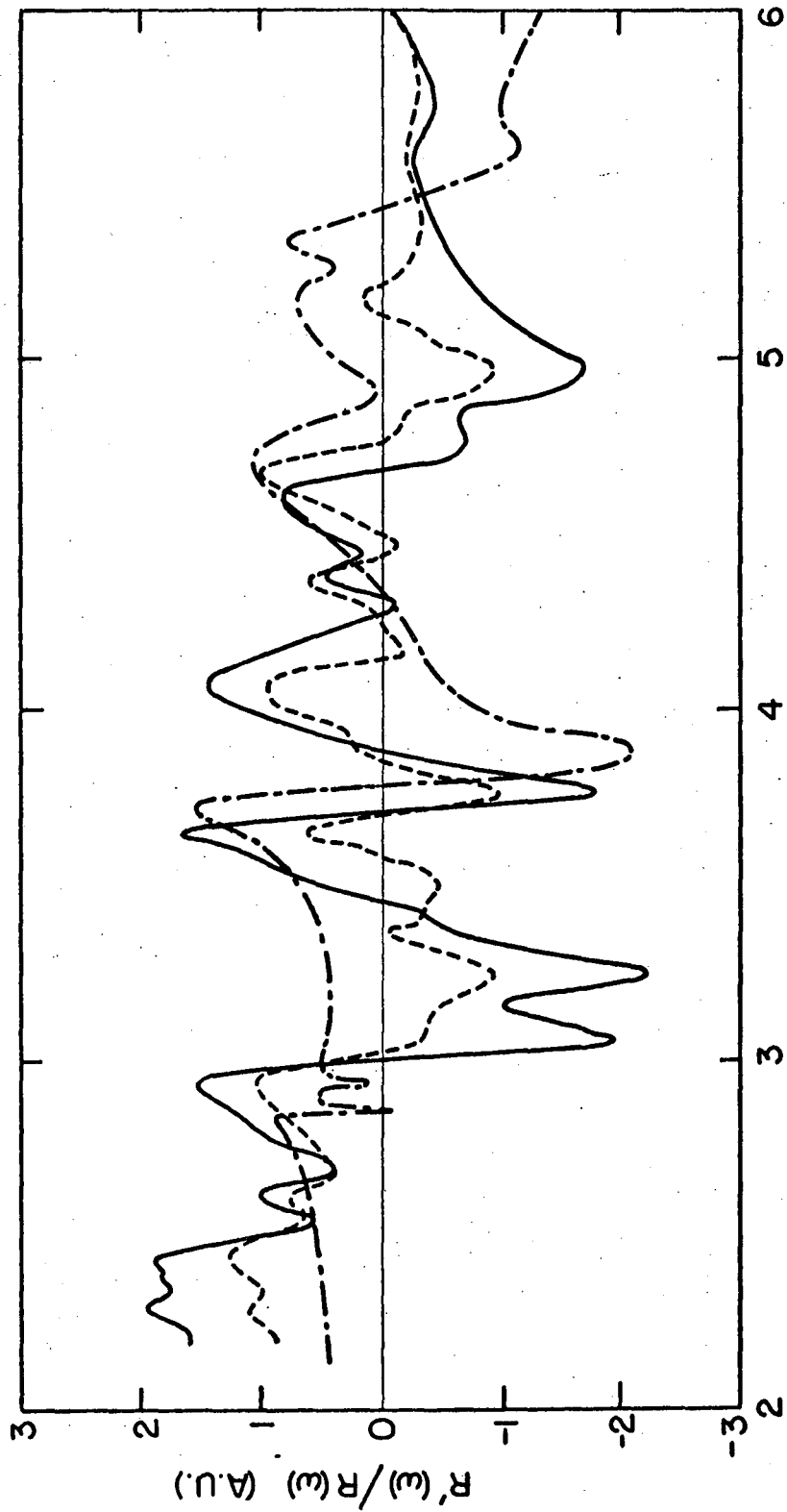
(d) Electromoreflectance work of Shay at 300°K (Ref. 14)

† Wavelength-modulated absorption work of Shileika at 77°K (Ref. 16)

\* spin-orbit Hamiltonian included.

Figure Captions

- Fig. 1. Derivative spectra  $1/R \, dR/d\omega$  of  $\text{ZnGeP}_2$  at  $5^\circ\text{K}$  for parallel (—) and perpendicular (--) polarization. For comparison the derivative spectra of GaP (---) is given.
- Fig. 2. Reflectivity of  $\text{ZnGeP}_2$  at  $5^\circ\text{K}$  and at  $300^\circ\text{K}$ .
- Fig. 3. Crystal structure of  $\text{ZnGeP}_2$ .
- Fig. 4. Band structure for  $\text{ZnGeP}_2$  along the principal symmetry directions.
- Fig. 5. Theoretical  $\epsilon_2(\omega)$  for  $\text{ZnGeP}_2$  for light polarized parallel and perpendicular to the c-axis of the crystal.
- Fig. 6. Comparison of the theoretical and experimental  $R(\omega)$  for  $\text{ZnGeP}_2$  in the parallel and perpendicular polarizations.

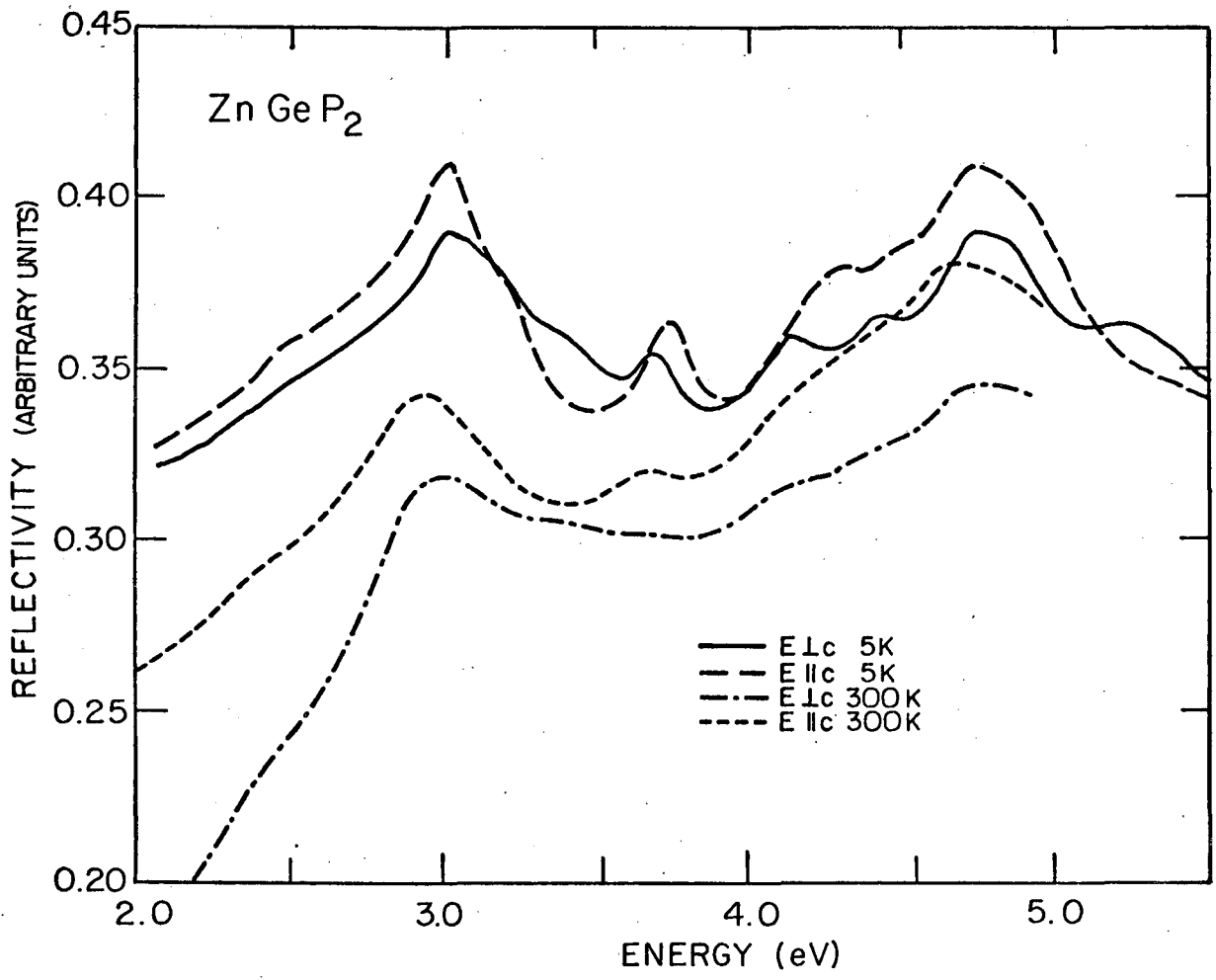


XBL 739-1250

Energy (eV)

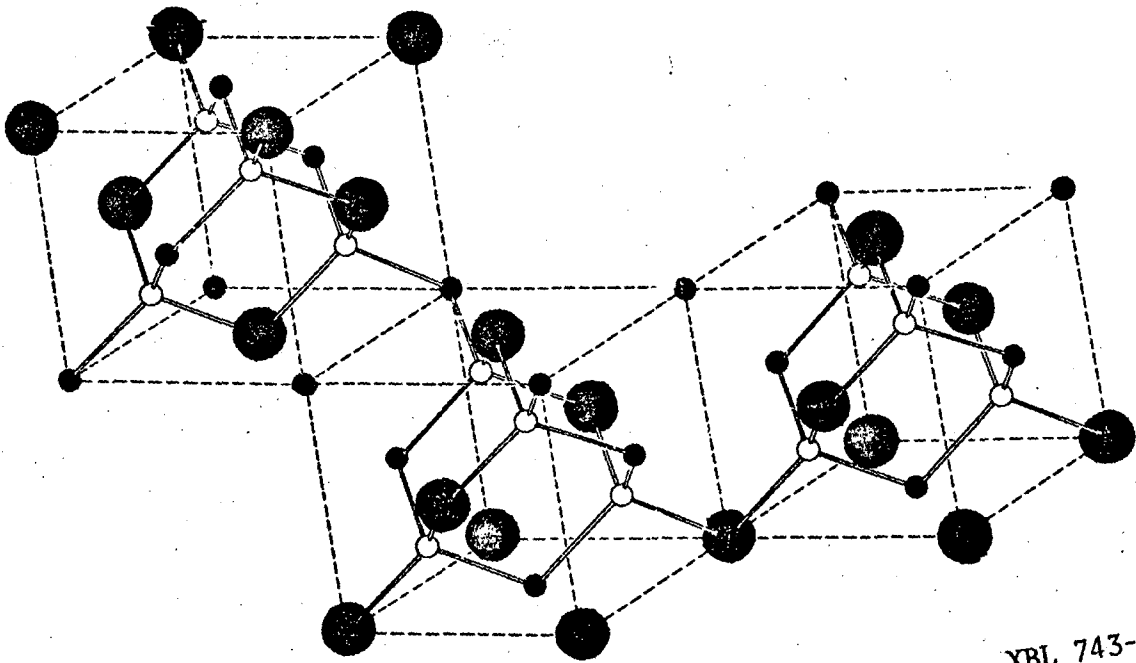
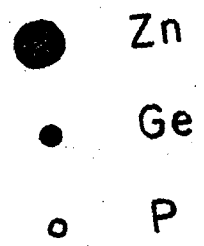
Figure 1





XBL743-5783

Figure 2.



XBL 743-5797

Figure 3

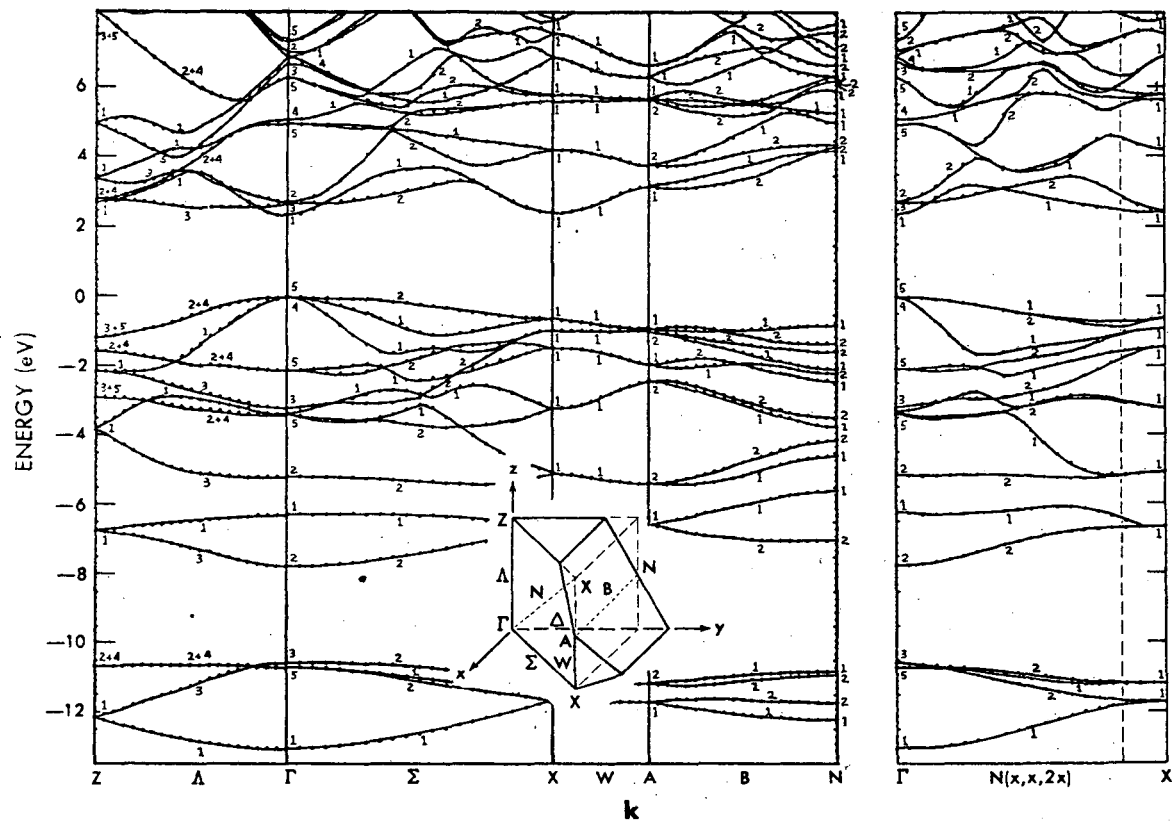
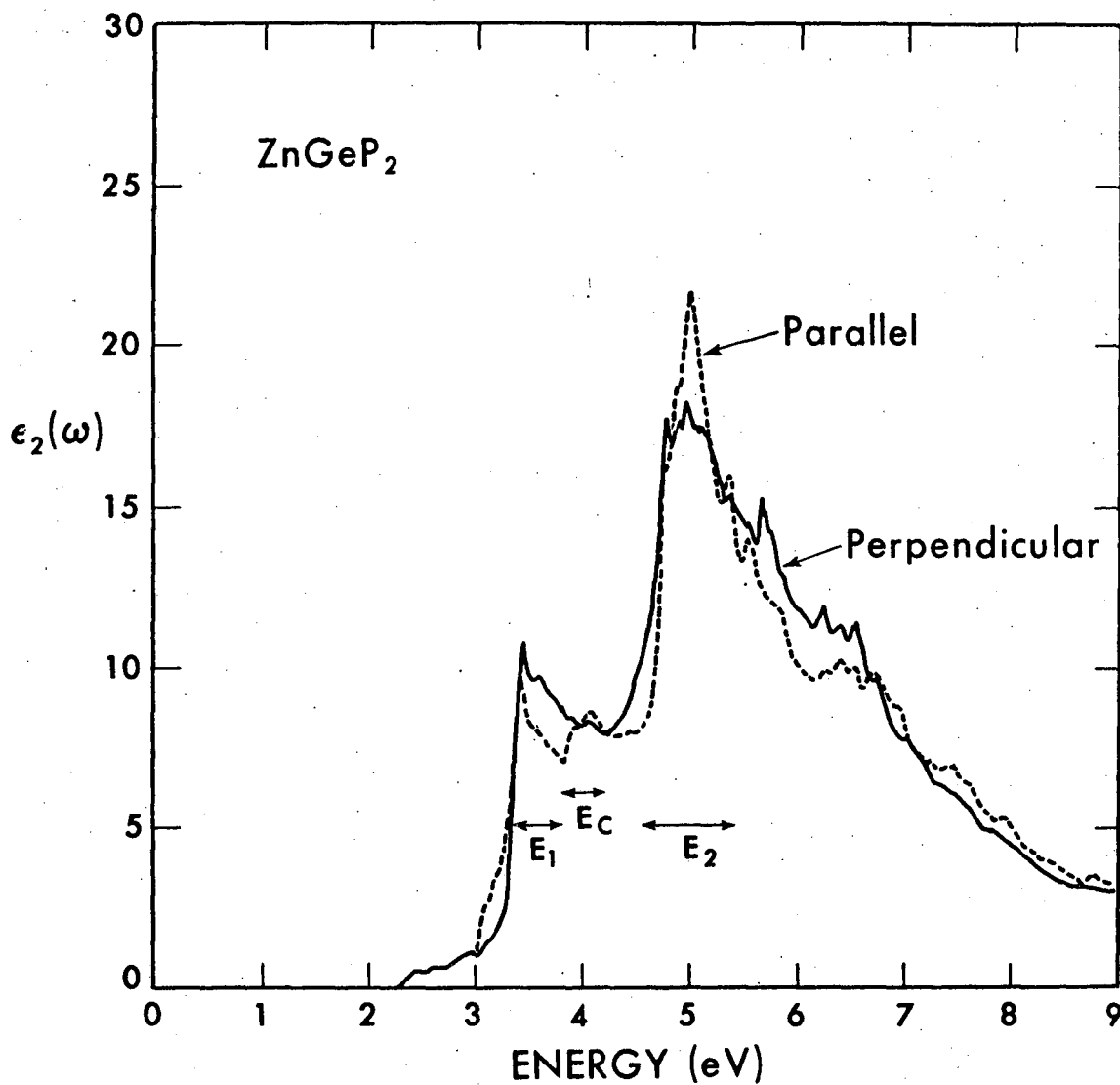
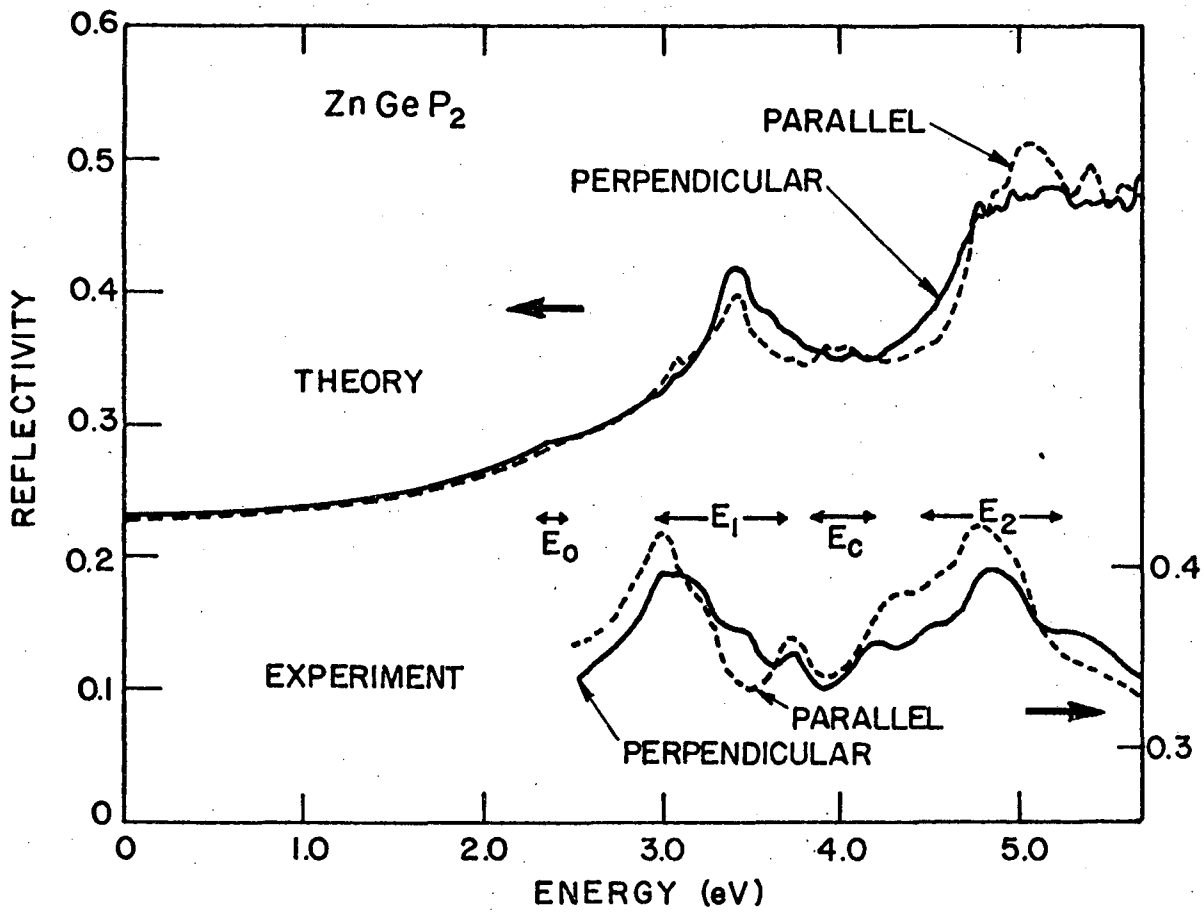


Figure 4



XBL 737-6599

Figure 5



XBL 738-1762

Figure 6

LEGAL NOTICE

*This report was prepared as an account of work sponsored by the United States Government. Neither the United States nor the United States Atomic Energy Commission, nor any of their employees, nor any of their contractors, subcontractors, or their employees, makes any warranty, express or implied, or assumes any legal liability or responsibility for the accuracy, completeness or usefulness of any information, apparatus, product or process disclosed, or represents that its use would not infringe privately owned rights.*

TECHNICAL INFORMATION DIVISION  
LAWRENCE BERKELEY LABORATORY  
UNIVERSITY OF CALIFORNIA  
BERKELEY, CALIFORNIA 94720